**J. Cent. South Univ.** (2013) 20: 2593−2598
**DOI:** 10.1007/s11771-013-1773-7

Springer

# Seismic stability of reinforced soil walls under bearing capacity failure by pseudo-dynamic method

RUAN Xiao-bo(阮晓波)[1], SUN Shu-lin(孙树林)[2]

1. College of Civil and Transportation Engineering, Hohai University, Nanjing 210098, China;
2. College of Earth Sciences and Engineering, Hohai University, Nanjing 210098, China;

© Central South University Press and Springer-Verlag Berlin Heidelberg 2013

**Abstract:** In order to evaluate the seismic stability of reinforced soil walls against bearing capacity failure, the seismic safety factor of reinforced soil walls was determined by using pseudo-dynamic method, and calculated by considering different parameters, such as horizontal and vertical seismic acceleration coefficients, ratio of reinforcement length to wall height, back fill friction angle, foundation soil friction angle, soil−reinforcement interface friction angle and surcharge. The parametric study shows that the seismic safety factor increases by 24-fold when the foundation soil friction angle varies from 25° to 45°, and increases by 2-fold when the soil−reinforcement interface friction angle varies from 0 to 30°. That is to say, the bigger values the foundation soil and/or soil−reinforcement interface friction angles have, the safer the reinforced soil walls become in the seismic design. The results were also compared with those obtained from pseudo-static method. It is found that there is a higher value of the safety factor by the present work.

**Key words:** reinforced soil walls; seismic stability against bearing capacity; seismic active force; pseudo-dynamic method

## 1 Introduction

During the design of reinforced soil walls in seismic prone zones, it is very important to study the external seismic stability of reinforced soil walls. The external stability evaluations of reinforced soil walls treat the reinforced section as a composite homogeneous soil mass, and usually consider four failure modes, viz., sliding, overturning, eccentricity and bearing capacity failure modes [1]. BASHA and BASUDHAR [2] assessed the external seismic stability of reinforced soil walls by using the pseudo-static method. However, in the pseudo-static method, the dynamic nature of seismic loading is considered to be time-independent, which assumes that the magnitude and phase acceleration are uniform throughout the reinforced section and back fill. To overcome this drawback, CHOUDHURY et al [3] determined the external seismic stability of reinforced soil walls by using the pseudo-dynamic method, but only considered direct sliding failure mode.

The pseudo-dynamic method was proposed by STEEDMAN and ZENG [4], and initially, only considered horizontal seismic acceleration. Then, ZENG and STEEDMAN [5] validated the pseudo-dynamic method by comparing the values with centrifuge model test results. In order to improve STEEDMAN and ZENG's method, CHOUDHURY and NIMBALKAR [6−8], and NIMBALKAR and CHOUDHURY [9] studied the seismic earth pressure on the retaining wall with the consideration of both horizontal and vertical seismic accelerations. However, the above-mentioned methods were merely applied to the vertical retaining wall. To analyze the nonvertical retaining wall, GHOSH [10−12] and WANG et al [13] calculated the seismic earth pressure behind it by the pseudo-dynamic method. In addition, WANG et al [13] also determined the safety factor of the retaining wall against overturning failure mode, but the surcharge was ignored.

Although the pseudo-dynamic method has been used to analyze the external seismic stability of reinforced soil walls, the seismic stability of reinforced soil walls against bearing capacity failure mode cannot be obtained. Thus, in this work, an expression for computing the seismic safety factor of reinforced soil walls against bearing capacity failure mode is provided. The effects of various parameters such as horizontal and vertical seismic acceleration coefficients ($k_h$ and $k_v$), ratio of reinforcement length to wall height ($L/H$), back fill friction angle ($\phi_b$), foundation soil friction angle ($\phi_f$), soil−reinforcement interface friction angle ($\delta$), and surcharge ($q$) on the seismic safety factor of reinforced

**Received date:** 2012−04−16; **Accepted date:** 2012−09−18
**Corresponding author:** RUAN Xiao-bo, PhD Candidate; Tel: +86−15905173242; E-mail: ruanxiaobo@hhu.edu.cn

soil walls are studied. This can provide valuable reference for seismic design of reinforced soil walls against bearing capacity failure.

## 2 Method of analysis

### 2.1 Pseudo-dynamic method

The pseudo-dynamic method considers finite shear and primary waves, and assumes that the shear moduli of reinforced soil, $G_r$, and of back fill, $G_b$, are constant with the depth, $z$, through the reinforced section and back fill. In the present analysis, the shear wave velocity, $V_{sr}=(G_r/\rho_r)^{0.5}$, where $\rho_r$ is the density of the reinforced soil, and primary wave velocity, $V_{pr}=(G_r(2-2\upsilon_r)/(\rho_r(1-2\upsilon_r)))^{0.5}$, where $\upsilon_r$ is the Poisson ratio of the reinforced soil, are assumed to act within the reinforced section due to seismic loading. Similarly, the shear and primary wave velocities acting within the back fill can be given by $V_{sb}=(G_b/\rho_b)^{0.5}$ and $V_{pb}=(G_b(2-2\upsilon_b)/(\rho_b(1-2\upsilon_b)))^{0.5}$, respectively, where $\rho_b$ is the density of the back fill and $\upsilon_b$ is the Poisson ratio of the back fill. For most geological materials, $V_{pr}/V_{sr}$ and $V_{pb}/V_{sb}$ can be taken as 1.87 [14]. The period of lateral shaking, $T=2\pi/\omega$, where $\omega$ is the angular frequency, is considered in the analysis. For most geotechnical structures, $T$=0.3 s is a reasonable assumption [15].

For a sinusoidal base shaking subjected to both horizontal and vertical seismic accelerations with the amplitude $k_hg$ and $k_vg$, where $k_h$ and $k_v$ are the horizontal and vertical seismic acceleration coefficients, respectively, the acceleration at any depth, $z$, below the ground surface and duration of earthquake, $t$, can be expressed as

$$a_{h1}(z,t)=k_h g\sin\omega\left(t-\frac{H+z_{q1}-z}{V_{sr}}\right) \tag{1}$$

$$a_{v1}(z,t)=k_v g\sin\omega\left(t-\frac{H+z_{q1}-z}{V_{pr}}\right) \tag{2}$$

$$a_{h2}(z,t)=k_h g\sin\omega\left(t-\frac{H+z_{q2}-z}{V_{sb}}\right) \tag{3}$$

$$a_{v2}(z,t)=k_v g\sin\omega\left(t-\frac{H+z_{q2}-z}{V_{pb}}\right) \tag{4}$$

where $z_{q1}=q/\gamma_r$ and $z_{q2}=q/\gamma_b$ are equivalent surcharge heights of reinforced soil mass and back fill wedge, respectively; $\gamma_r$ and $\gamma_b$ are unit weights of reinforced soil and back fill, respectively.

Figure 1 depicts the schematic diagram of reinforced soil walls and forces involved in bearing capacity failure condition, and Fig. 2 illustrates the failure mechanism of back fill and associated forces.

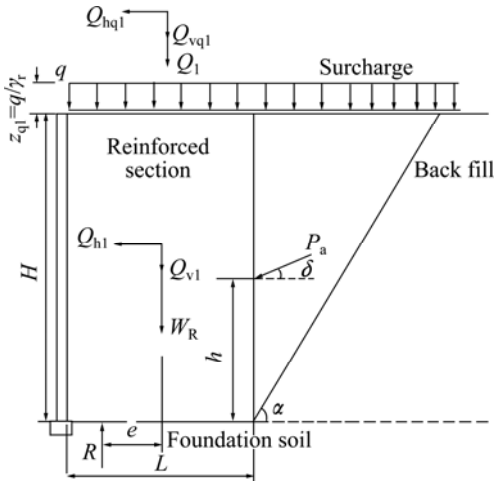


**Fig. 1** Schematic diagram of reinforced soil walls and forces involved in bearing capacity failure condition

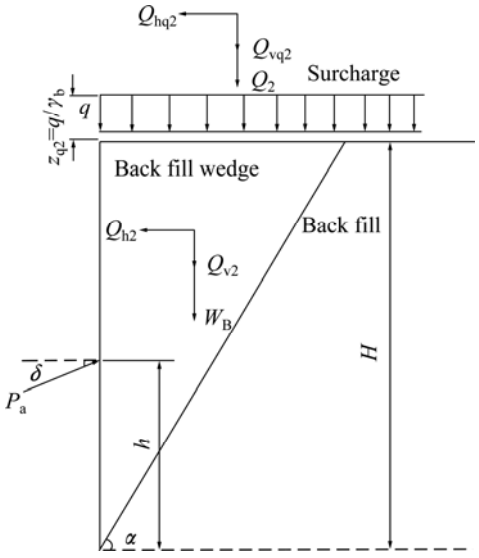


**Fig. 2** Failure mechanism of backfill and associated forces

### 2.2 Seismic active force acting on reinforced section

The weight of the back fill wedge is

$$W_B=\frac{1}{2}\gamma_b H^2\cot\alpha \tag{5}$$

where $\alpha$ is failure angle of the back fill, and $H$ is height of reinforced soil walls.

The total surcharge acting on the back fill is

$$Q_2=qH\cot\alpha \tag{6}$$

where $q$ is surcharge.

The total horizontal seismic force acting on the back fill wedge and surcharge, respectively, can be obtained by

$$Q_{h2}=\frac{k_h\lambda_b\gamma_b\cot\alpha}{2\pi}\left[H\cos 2\pi\left(\frac{t}{T}-\frac{H}{\lambda_b}\right)-\frac{\lambda_b}{2\pi}\times\left(\sin 2\pi\left(\frac{t}{T}\right)-\sin 2\pi\left(\frac{t}{T}-\frac{H}{\lambda_b}\right)\right)\right] \tag{7}$$

$$Q_{\mathrm{hq2}}=\frac{k_{\mathrm{h}}\lambda_{\mathrm{b}}qH\cot\alpha}{2\pi z_{\mathrm{q2}}}\left[\cos 2\pi\left(\frac{t}{T}-\frac{H+z_{\mathrm{q2}}}{\lambda_{\mathrm{b}}}\right)-\cos 2\pi\left(\frac{t}{T}-\frac{H}{\lambda_{\mathrm{b}}}\right)\right] \tag{8}$$

where $\lambda_{\mathrm{b}}=TV_{\mathrm{sb}}$, is the wavelength of shear wave about back fill.

Similarly, the total vertical seismic force acting on the back fill wedge and surcharge, respectively, can also be obtained by

$$Q_{\mathrm{v2}}=\frac{k_{\mathrm{v}}\eta_{\mathrm{b}}\gamma_{\mathrm{b}}\cot\alpha}{2\pi}\left[H\cos 2\pi\left(\frac{t}{T}-\frac{H}{\eta_{\mathrm{b}}}\right)-\frac{\eta_{\mathrm{b}}}{2\pi}\times\left(\sin 2\pi\left(\frac{t}{T}\right)-\sin 2\pi\left(\frac{t}{T}-\frac{H}{\eta_{\mathrm{b}}}\right)\right)\right] \tag{9}$$

$$Q_{\mathrm{vq2}}=\frac{k_{\mathrm{v}}\eta_{\mathrm{b}}qH\cot\alpha}{2\pi z_{\mathrm{q2}}}\left[\cos 2\pi\left(\frac{t}{T}-\frac{H+z_{\mathrm{q2}}}{\eta_{\mathrm{b}}}\right)-\cos 2\pi\left(\frac{t}{T}-\frac{H}{\eta_{\mathrm{b}}}\right)\right] \tag{10}$$

where $\eta_{\mathrm{b}}=TV_{\mathrm{pb}}$, is the wavelength of primary wave about back fill.

The total seismic active earth pressure, $P_{\mathrm{a}}(t)$, can be obtained by resolving the forces on the back fill wedge and considering the equilibrium of the forces, hence, $P_{\mathrm{a}}(t)$ can be expressed as

$$P_{\mathrm{a}}(t)=\frac{\left(W_{\mathrm{B}}+Q_2+Q_{\mathrm{v2}}+Q_{\mathrm{vq2}}\right)\sin\left(\alpha-\phi_{\mathrm{b}}\right)}{\cos\left(\delta+\phi_{\mathrm{b}}-\alpha\right)}+\frac{\left(Q_{\mathrm{h2}}+Q_{\mathrm{hq2}}\right)\cos\left(\alpha-\phi_{\mathrm{b}}\right)}{\cos\left(\delta+\phi_{\mathrm{b}}-\alpha\right)} \tag{11}$$

The seismic active earth pressure distribution can be obtained by differentiating $P_{\mathrm{a}}(z,t)$ with respect to the depth, $z$, as

$$p_{\mathrm{a}}(z,t)=\frac{\partial P_{\mathrm{a}}(z,t)}{\partial z}=\left\{\gamma_{\mathrm{b}}\left(z-z_{\mathrm{q2}}\right)\cot\alpha+q\cot\alpha+k_{\mathrm{v}}\gamma_{\mathrm{b}}\cot\alpha\left(z-z_{\mathrm{q2}}\right)d_{\eta 1}+\frac{k_{\mathrm{v}}\eta_{\mathrm{b}}q\cot\alpha}{2\pi z_{\mathrm{q2}}}\left[d_{\eta 2}+\frac{2\pi\left(z-z_{\mathrm{q2}}\right)d_{\eta 3}}{\eta_{\mathrm{b}}}\right]\right\}\frac{\sin\left(\alpha-\phi_{\mathrm{b}}\right)}{\cos\left(\delta+\phi_{\mathrm{b}}-\alpha\right)}+\left\{k_{\mathrm{h}}\gamma_{\mathrm{b}}\cot\alpha\left(z-z_{\mathrm{q2}}\right)d_{\lambda 1}+\frac{k_{\mathrm{h}}\lambda_{\mathrm{b}}q\cot\alpha}{2\pi z_{\mathrm{q2}}}\left[d_{\lambda 2}+\frac{2\pi\left(z-z_{\mathrm{q2}}\right)d_{\lambda 3}}{\lambda_{\mathrm{b}}}\right]\right\}\frac{\cos\left(\alpha-\phi_{\mathrm{b}}\right)}{\cos\left(\delta+\phi_{\mathrm{b}}-\alpha\right)} \tag{12}$$

where $d_{\eta 1}=\sin 2\pi(t/T-(z-z_{\mathrm{q2}})/\eta_{\mathrm{b}})$; $d_{\eta 2}=\cos 2\pi(t/T-z/\eta_{\mathrm{b}})-\cos 2\pi(t/T-(z-z_{\mathrm{q2}})/\eta_{\mathrm{b}})$; $d_{\eta 3}=\sin 2\pi(t/T-z/\eta_{\mathrm{b}})-\sin 2\pi(t/T-(z-z_{\mathrm{q2}})/\eta_{\mathrm{b}})$; $d_{\lambda 1}=\sin 2\pi(t/T-(z-z_{\mathrm{q2}})/\lambda_{\mathrm{b}})$; $d_{\lambda 2}=\cos 2\pi(t/T-z/\lambda_{\mathrm{b}})-\cos 2\pi(t/T-(z-z_{\mathrm{q2}})/\lambda_{\mathrm{b}})$; $d_{\lambda 3}=\sin 2\pi(t/T-z/\lambda_{\mathrm{b}})-\sin 2\pi(t/T-(z-z_{\mathrm{q2}})/\lambda_{\mathrm{b}})$.

The acting point of seismic active earth pressure, $h$, can be determined by taking moment equilibrium about the base of the wall:

$$h=\frac{\int_0^{H+z_{\mathrm{q2}}}\left(H+z_{\mathrm{q2}}-z\right)p_{\mathrm{a}}(z,t)\mathrm{d}z}{P_{\mathrm{a}}(t)} \tag{13}$$

The total active earth pressure will be maximum when the failure angle is obtained by taking partial derivative of $P_{\mathrm{a}}(\alpha, t)$ with respective to failure angle, $\alpha$, which is called as the critical failure angle, $\alpha_{\mathrm{c}}$ [16−18]:

$$\frac{\partial P_{\mathrm{a}}(\alpha,t)}{\partial\alpha}=0 \tag{14}$$

Simplification of Eq. (14) can be given by

$$\left[a\cos\left(2\alpha_{\mathrm{c}}-\phi_{\mathrm{b}}\right)-b\sin\left(2\alpha_{\mathrm{c}}-\phi_{\mathrm{b}}\right)\right]\times\sin\alpha_{\mathrm{c}}\cos\left(\delta+\phi_{\mathrm{b}}-\alpha_{\mathrm{c}}\right)-\left[a\sin\left(\alpha_{\mathrm{c}}-\phi_{\mathrm{b}}\right)+b\cos\left(\alpha_{\mathrm{c}}-\phi_{\mathrm{b}}\right)\right]\times\cos\alpha_{\mathrm{c}}\cos\left(\delta+\phi_{\mathrm{b}}\right)=0 \tag{15}$$

where $a=0.5\gamma_{\mathrm{b}}H^2+qH+k_{\mathrm{v}}\eta_{\mathrm{b}}\gamma_{\mathrm{b}}[H\cos 2\pi(t/T-H/\eta_{\mathrm{b}})-\eta_{\mathrm{b}}(\sin 2\pi(t/T)-\sin 2\pi(t/T-H/\eta_{\mathrm{b}}))/2\pi]/2\pi+k_{\mathrm{v}}\eta_{\mathrm{b}}qH[\cos 2\pi(t/T-(H+z_{\mathrm{q2}})/\eta_{\mathrm{b}})-\cos 2\pi(t/T-H/\eta_{\mathrm{b}})]/(2\pi z_{\mathrm{q2}})$

$b=k_{\mathrm{h}}\lambda_{\mathrm{b}}\gamma_{\mathrm{b}}[H\cos 2\pi(t/T-H/\lambda_{\mathrm{b}})-\lambda_{\mathrm{b}}(\sin 2\pi(t/T)-\sin 2\pi(t/T-H/\lambda_{\mathrm{b}}))/2\pi]/2\pi+k_{\mathrm{h}}\lambda_{\mathrm{b}}qH[\cos 2\pi(t/T-(H+z_{\mathrm{q2}})/\lambda_{\mathrm{b}})-\cos 2\pi(t/T-H/\lambda_{\mathrm{b}})]/(2\pi z_{\mathrm{q2}})$

The critical failure angle, $a_{\mathrm{c}}$, can be obtained by solving Eq. (15).

### 2.3 Seismic safety factor against bearing capacity failure mode

The weight of the reinforced soil mass is

$$W_{\mathrm{R}}=\gamma_{\mathrm{r}}HL \tag{16}$$

where $L$ is reinforcement length.

The total surcharge acting on the reinforced section is

$$Q_{\mathrm{l}}=qL \tag{17}$$

The total horizontal seismic force acting on the reinforced section and surcharge, respectively, can be given by

$$Q_{\mathrm{h1}}=\frac{k_{\mathrm{h}}\lambda_{\mathrm{r}}\gamma_{\mathrm{r}}L}{2\pi}\left[\cos 2\pi\left(\frac{t}{T}-\frac{H}{\lambda_{\mathrm{r}}}\right)-\cos 2\pi\left(\frac{t}{T}\right)\right] \tag{18}$$

$$Q_{\mathrm{hq1}}=\frac{k_{\mathrm{h}}\lambda_{\mathrm{r}}qL}{2\pi z_{\mathrm{q1}}}\left[\cos 2\pi\left(\frac{t}{T}-\frac{H+z_{\mathrm{q1}}}{\lambda_{\mathrm{r}}}\right)-\cos 2\pi\left(\frac{t}{T}-\frac{H}{\lambda_{\mathrm{r}}}\right)\right] \tag{19}$$

where $\lambda_r=TV_{sr}$, is the wavelength of shear wave about reinforced soil.

Similarly, the total vertical seismic force acting on the reinforced section and surcharge, respectively, can also be given by

$$Q_{v1}=\frac{k_v\eta_r\gamma_r L}{2\pi}\left[\cos 2\pi\left(\frac{t}{T}-\frac{H}{\eta_r}\right)-\cos 2\pi\left(\frac{t}{T}\right)\right] \tag{20}$$

$$Q_{vq1}=\frac{k_v\eta_r qL}{2\pi z_{q1}}\left[\cos 2\pi\left(\frac{t}{T}-\frac{H+z_{q1}}{\eta_r}\right)-\cos 2\pi\left(\frac{t}{T}-\frac{H}{\eta_r}\right)\right] \tag{21}$$

where $\eta_r=TV_{pr}$, is the wavelength of primary wave about reinforced soil.

The eccentricity can be calculated as the ratio of difference of sum of the moments of resisting forces to disturbing forces about the center line of the wall base as shown in the following equation:

$$E=\frac{Q_{h1}H/2+Q_{hq1}\left(H+z_{q1}/2\right)+(P_a\cos\delta)h}{R}-\frac{(P_a\sin\delta)L/2}{R} \tag{22}$$

where $R=W_R+Q_1+Q_{v1}+Q_{vq1}+P_a\sin\delta$, is the normal force at the base.

Bearing capacity refers to the ability of a foundation soil to support the structure. The Meyerhof distribution assumes that eccentric loading results in a uniform redistribution of pressure over a reduced area at the base of the wall. This area is defined by a width equal to the wall width minus twice the eccentricity. The safety factor against the bearing capacity failure can be defined by the ratio of ultimate bearing capacity of a shallow foundation below the base slab of reinforced soil, $q_u$, to vertical stress at the base, $\sigma_v$, as shown below [1, 14]:

$$F_S=\frac{q_u}{\sigma_v} \tag{23}$$

where $\sigma_v=R/(L-2E)$, $q_u=0.5\gamma_f(L-2E)N_\gamma$, and $\gamma_f$ is unit weight of foundation soil; $N_\gamma=2(N_q+1)\tan\phi_f$, is bearing capacity factor; $N_q=\exp(\pi\tan\phi_f)\tan(\pi/4+\phi_f/2)$; $\phi_f$ is foundation soil friction angle.

## 3 Results and discussion

In the case of cohesionless soils, to avoid the phenomenon of shear fluidization for the certain combinations of $k_h$ and $k_v$, RICHARDS et al [19] proposed that the soil friction angle, $\phi$, considered in the analysis has to satisfy the following relationship:

$$\phi > \tan^{-1}\left(\frac{k_h}{1-k_v}\right) \tag{24}$$

In order to investigate the effect of various parameters on the seismic safety factor of reinforced soil walls against bearing capacity failure, the range of parameters and its basic values considered in the analysis are presented in Table 1, and the downward seismic force is defined as positive.

**Table 1** Range of parameters and its basic values considered in present work

| Parameter | Basic value | Range |
|---|---|---|
| $H$/m | 10 | — |
| $q$/(kN·m$^{-2}$) | 10 | 5−20 |
| $L/H$ | 0.6 | 0.5−0.7 |
| $\phi_b$/(°) | 35 | 25−35 |
| $\phi_r$/(°) | 35 | — |
| $\phi_f$/(°) | 35 | 25−35 |
| $\delta$/(°) | 20 | 0−30 |
| $t$/s | 0.3 | — |
| $k_h$ | — | 0−0.4 |
| $k_v$ | 0.5 $k_h$ | −0.3− + 0.3 |
| ($\gamma_b=\gamma_r=\gamma_f$)/(kN·m$^{-3}$) | 18 | — |
| ($V_{sr}=V_{sb}$)/(m·s$^{-1}$) | 200 | — |

Figure 3 shows the variations of the safety factor of reinforced soil walls, $F_S$, with $k_h$ for different values of $L/H$ and $k_v$=0. It can be seen from Fig. 3 that $F_S$ decreases with the increase of $k_h$.

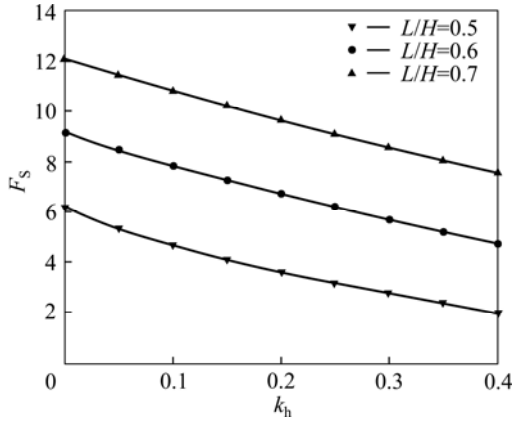


**Fig. 3** Variations of safety factor of reinforced soil walls, $F_S$, with $k_h$ for different values of $L/H$

Figure 4 depicts the variations of the safety factor of reinforced soil walls, $F_S$, with $k_v$ for different values of $L/H$ and $k_h$=0.3. It is indicated in Fig. 4 that $F_S$ decreases with the increase of $k_v$. When $L/H$ is equal to 0.5, the variation of $F_S$ is not obvious with the increase of $k_v$. However, the variation of $F_S$ begins to become apparent with the increase of $k_v$ when $L/H$ is greater than 0.5. It can be also seen from Fig. 4 that the impact of the downward seismic force on the stability of reinforced soil walls is more adverse.

Figures 3 and 4 also indicate that $F_S$ increases

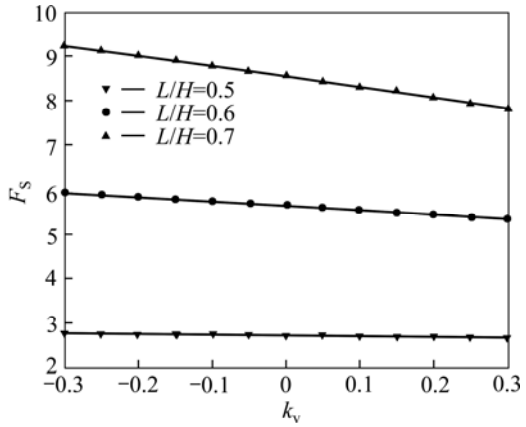


**Fig. 4** Variations of safety factor of reinforced soil walls, $F_S$, with $k_v$ for different values of $L/H$

rapidly with the increase of $L/H$. To make the following parameter research, $L/H$ is assumed to be equal to 0.6, and the downward seismic force is only considered.

Figure 5 shows the variations of the safety factor of reinforced soil walls, $F_S$, with $k_h$ for different values of $\phi_b$. Figure 5 indicates that $F_S$ decreases gradually with the increase of $k_h$, and increases obviously with the increase of $\phi_b$. When $\phi_b$ varies from 25° to 45°, $F_S$ increases from 3.579 to 6.813 for $k_h$ =0.3, and increases by 90%.

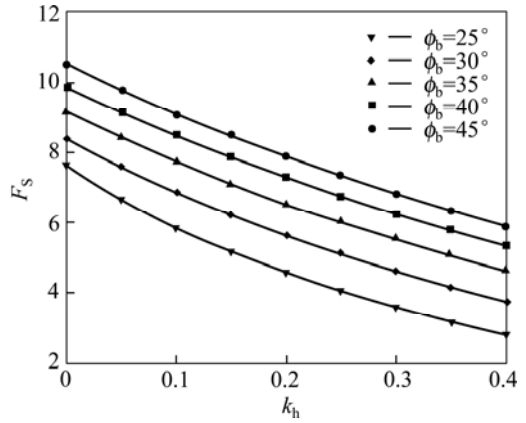


**Fig. 5** Variations of safety factor of reinforced soil walls, $F_S$, with $k_h$ for different values of $\phi_b$

Figure 6 shows the variations of the safety factor of reinforced soil walls, $F_S$, with $k_h$ for different values of $\phi_f$. It is observed in Fig. 6 that $F_S$ decreases significantly with the increase of $k_h$ when $\phi_f$ has a larger value, and increases strongly with the increase of $\phi_f$. When $\phi_f$ varies from 25° to 45°, $F_S$ increases from 1.245 to 31.099 for $k_h$=0.3, and increases by 24-fold.

Figure 7 shows the variations of the safety factor of reinforced soil walls, $F_S$, with $k_h$ for different values of $\delta$. Figure 7 demonstrates that $F_S$ decreases gradually with the increase of $k_h$, and increases clearly with the increase of $\delta$. When $\delta$ is changed from 0 to 30°, $F_S$ increases from 2.226 to 6.490 for $k_h$ =0.3, and increases by 2-fold.

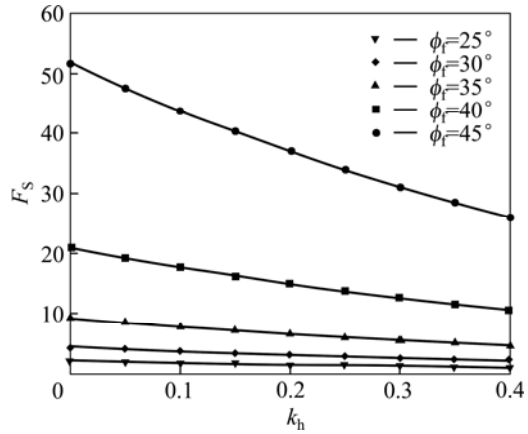


**Fig. 6** Variations of safety factor of reinforced soil walls, $F_S$, with $k_h$ for different values of $\phi_f$

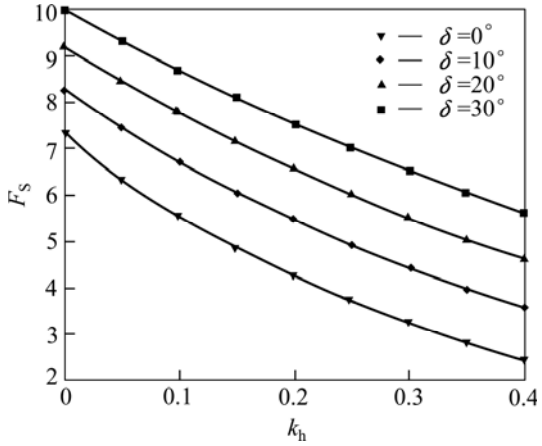


**Fig. 7** Variations of safety factor of reinforced soil walls, $F_S$, with $k_h$ for different values of $\delta$

Figure 8 shows the variations of the safety factor of reinforced soil walls, $F_S$, with $k_h$ for different values of $q$. It can be found in Fig. 8 that $F_S$ decreases quickly with the increase of $k_h$, and decrease slightly with the increase of $q$. When $q$ varies from 5 kN/m$^2$ to 20 kN/m$^2$, $F_S$ decreases from 5.826 to 4.839 for $k_h$=0.3, and decreases by 17%.

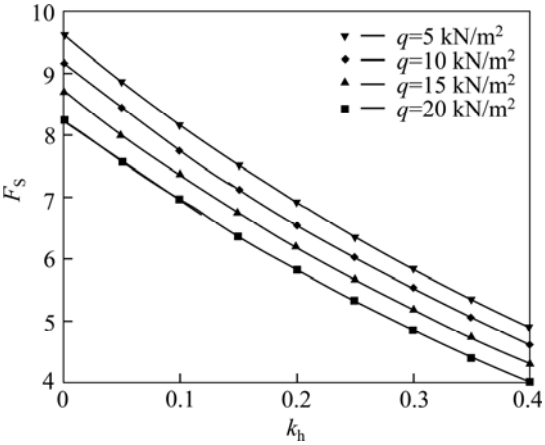


**Fig. 8** Variations of safety factor of reinforced soil walls, $F_S$, with $k_h$ for different values of $q$

## 4 Comparison of results

Figure 9 shows a comparison of safety factor obtained by the present study with that obtained from the pseudo-static method [2] for $k_v=k_h/2$, $H/\lambda_r=H/\lambda_b=0.3$, $H/\eta_r=H/\eta_b=0.16$. It is observed that the results obtained from the present study are larger than the results obtained from the pseudo-static method for the same set of parameters. Furthermore, the lager value the horizontal seismic force has, the more obvious the difference of the results between the present work and the pseudo-static method becomes.

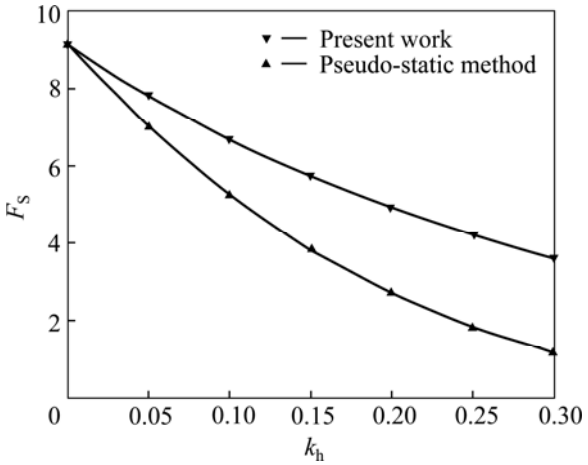


**Fig. 9** Comparisons of variation of safety factor of reinforced soil walls, $F_S$, with $k_h$ obtained by present study and pseudo-static method

## 5 Conclusions

1) The safety factor decreases with the increase of horizontal or vertical seismic acceleration coefficients. But, the horizontal seismic acceleration coefficient affects the safety factor more significantly, and the impact of the downward seismic force on the safety factor is more disadvantageous.

2) The safety factor increases gradually with the increase of the ratio of reinforcement length to wall height. In seismic design, the appropriate increase of the ratio of reinforcement length to wall height is conducive to the stability of reinforced soil walls.

3) The safety factor increases with the increase of back fill friction angle, foundation soil friction angle, and soil−reinforcement interface friction angle. In addition, the foundation soil friction angle has much stronger influence on the seismic stability of reinforced soil walls than the others.

4) The safety factor decreases slowly with the increase of surcharge. Therefore, the surcharge slightly affects the seismic stability of reinforced soil walls.

5) The results obtained from the pseudo-static method are more conservative than the results obtained from the present work in the same situation.

## References

[1] FHWA-NHI-00-043. Mechanically stabilized earth walls and reinforced soil slopes, design and construction guidelines [S]. Washington, DC, US: Department of Transportation, Federal Highway Administration (FHWA), 2001.

[2] BASHA B M, BASUDHAR P K. Pseudo static seismic stability analysis of reinforced soil structures [J]. Geotechnical and Geological Engineering, 2010, 28(6):745−762.

[3] CHOUDHURY D, NIMBALKAR S S, MANDAL J N. External stability of reinforced soil walls under seismic conditions [J]. Geosynthetics International, 2007, 14(4): 211−218.

[4] STEEDMAN R S, ZENG X. The influence of phase on the calculation of pseudo-static earth pressure on a retaining wall [J]. Geotechnique, 1990, 40(1): 103−112.

[5] ZENG X, STEEDMAN R S. On the behaviour of quay walls in earthquakes [J]. Geotechnique, 1993, 43(3): 417−431.

[6] CHOUDHURY D, NIMBALKAR S S. Seismic passive resistance by pseudo-dynamic method [J]. Geotechnique, 2005, 55(9): 699−702.

[7] CHOUDHURY D, NIMBALKAR S S. Pseudo-dynamic approach of seismic active earth pressure behind retaining wall [J]. Geotechnical and Geological Engineering, 2006, 24(5): 1103−1113.

[8] CHOUDHURY D, NIMBALKAR S S. Seismic rotational displacement of gravity walls by pseudo-dynamic method: Passive case [J]. Soil Dynamics and Earthquake Engineering, 2007, 27(3): 242−249.

[9] NIMBALKAR S S, CHOUDHURY D. Sliding stability and seismic design of retaining wall by pseudo-dynamic method for passive case [J]. Soil Dynamic Earthquake Engineering, 2007, 27(6): 497−505.

[10] GHOSH P. Seismic passive earth pressure behind non-vertical retaining wall using pseudo-dynamic analysis [J]. Geotechnical and Geological Engineering, 2007, 25(6): 693−703.

[11] GHOSH P. Seismic active earth pressure behind a nonvertical retaining wall using pseudo-dynamic analysis [J]. Canadian Geotechnical Journal, 2008, 45(9): 117−123.

[12] GHOSH S. Pseudo-dynamic active force and pressure behind battered retaining wall supporting inclined backfill [J]. Soil Dynamics and Earthquake Engineering, 2010, 30(11): 1226−1232.

[13] WANG Kui-hua, MA Shao-jun, WU Wen-bing. Pseudo-dynamic analysis of overturning stability of retaining wall [J]. Journal of Central South University of Technology, 2011, 18(6): 2085−2090.

[14] DAS B M, RAMANA G V. Principles of soil dynamics. 2nd Ed [M]. Connecticut: Stamford, Cengage Learning, 2010: 1−563.

[15] PRAKASH S. Soil dynamics [M]. New York: McGraw-Hill Book Company, 1981: 1−450.

[16] SHUKLA S K, GUPTA S K, SIVAKUGAN N. Active earth pressure on retaining wall for $c$-$\phi$ soil backfill under seismic loading condition [J]. Journal of Geotechnical and Geoenvironmental Engineering, 2009, 135(5): 690−696.

[17] SHUKLA S K. Dynamic active thrust from $c$-$\phi$ soil backfills [J]. Soil Dynamics and Earthquake Engineering, 2011, 31(3): 526−529.

[18] SHUKLA S K, HABIBI D. Dynamic passive pressure from $c$-$\phi$ soil backfills [J]. Soil Dynamics and Earthquake Engineering, 2011, 31(5/6): 845−848.

[19] RICHARDS R, ELMS D G, BUDHU M. Dynamic fluidization of soils [J]. Journal of Geotechnical Engineering, 1990, 116(5): 740−759.

**(Edited by YANG Bing)**